MDPI

Article

Comparison of Critical Shear Stress of Rill Erosion Estimated from Two Methods

Ren Geng [1,*], Qiu Jin [1,*], Shaohua Lei [1], Hongyuan Liu [2], Bin Lu [1] and Meixiang Xie [1]

1 Sate Key Laboratory of Hydrology-Water Resources and Hydraulic Engineering, Nanjing Hydraulic Research Institute, Nanjing 210029, China; shaohualei@nhri.cn (S.L.); blu@nhri.cn (B.L.); jsdyxmx@163.com (M.X.)
2 Key Laboratory of Wetland Ecology and Environment, Northeast Institute of Geography and Agroecology, Chinese Academy of Sciences, Changchun 130102, China; gladysxey53@gmail.com
* Correspondence: rgeng@nhri.cn (R.G.); nhrijq83@163.com (Q.J.)

Abstract: Various disputes exist regarding the critical shear stress (τ_c) of rill erosion determined by linear regression. Alternatively, some researchers have attempted to measure critical shear stress (τ_o) of rill erosion by observing the start of soil particle detachment and showed promising results. However, few studies have been conducted to evaluate the reliability of the method determining τ_o. Thus, this study was conducted to identify the reliability of the method determining τ_o by comparing the values of τ_c and τ_o and their relationships with rill erodibility (K_r) and influencing factors, using 360 disturbed soil samples (standing for the freshly tilled condition) from six sampling sites along a 330 km transect in the Loess Plateau. Results indicated that the mean τ_c was 1.90 times greater than that of τ_o. No significant relationship was found between τ_c and K_r. An inverse changing trend between K_r and τ_o was observed from Yijun to Zizhou, while both K_r and τ_o exhibited increasing trends from Zizhou to Yulin. The τ_o of six sampling sites all demonstrated increasing trends with slope gradient (S), which contradicted the statement of the WEPP model that τ_c was independent of S. The relationships between τ_c and the measured soil properties were poor, whereas the τ_o increased exponentially with soil organic matter. Generally, τ_o did not present significantly better results than τ_c; the reliability of τ_o also showed some uncertainties, such as the subjective judgment of the beginning detachment of soil particles. This result has great importance for deepening our understanding of the rill erosion mechanism.

Keywords: soil erosion; critical shear stress; rill erodibility; soil detachment capacity; Loess Plateau

1. Introduction

Soil erosion by water leads to land degradation, reduced crop yields, water pollution, threatening biodiversity and sustainability of environmentally protected areas, and other problems, which have made it a serious global problem [1–5]. A soil erosion model is essential for understanding the erosion process and implementing effective soil conservation measures [6–8]. The Universal Soil Loess Equation (ULSE) and revised ULSE (RULSE) were widely applied to predict soil erosion [5]. However, ULSE and RUSLE were empirical and lacked deep recognition of erosion processes and erosion mechanisms [5,8]. Thus, many studies in recent decades have been concerned with process-based models, which were physically-based and could model erosion processes [9,10]. In these models, represented by the Water Erosion Prediction Project (WEPP), the rill erosion of overland flow is the most important process that influences sediment production [11]. Rill erodibility (K_r, s m^{-1}) and critical shear stress (τ_c, Pa) (both refer to soil resistance to overland flow) are crucial parameters for modeling rill erosion [7]. K_r and τ_c are usually determined by the linear regression of soil detachment capacity (D_c, kg m^{-2} s^{-1}) and flow shear stress (τ, Pa) [12].

Generally, K_r and τ_c are greatly influenced by soil properties (such as soil texture, soil cohesion, soil organic matter (SOM), plant roots, etc.) [13–15].

In past decades, researchers have done significant work on the influencing factors of K_r and have reached a consensus about the effects of these influencing factors on K_r [16–18]). Soil texture was widely used in the prediction of K_r [16]. Geng et al. [18] studied the response of K_r to landscape positions in a small watershed and found K_r decreased and increased with increasing clay content and sand content, respectively. Soil cohesion reflects the cohesive forces among soil particles [19]. Wang et al. [20] found a negative relationship between K_r and soil cohesion. SOM affects soil resistance to overland flow by functioning as a cementing agent among soil particles [17]. Geng et al. [21] proposed a significant correlation between K_r and SOM. Plant roots also impose great influence on K_r due to their chemical bonding effect and physical bonding effect [14,22]. K_r usually increases exponentially with root mass density [20].

Significant disagreement remains, however, regarding other crucially important parameters of soil resistance to overland, namely τ_c [23,24]. Generally speaking, these disagreements can be categorized as follows: (1) Unlike K_r, the relationships between τ_c and its potential influencing factors were rather confusing [21,25]. For example, Gilly et al. [25] quantified the τ_c of 36 soils throughout the United States and indicated that τ_c could be predicted by clay content, linear extensibility coefficient, and soil water content. Nonetheless, Geng et al. [21] showed no significant relationship between τ_c and 17 measured soil properties for 36 soil types across Eastern China. (2) There is also no general agreement on the relationship between K_r and τ_c. Many studies indicated that soils with higher τ_c correspond to less erodibility [26,27]. Knapen et al. [17] found that no significant relationship existed between K_r and τ_c for both laboratory ($n = 179$) and field experiments ($n = 151$). Additionally, Mamo and Bubenzer's [27] findings did not support the opinion that when τ_c was smaller, K_r would be larger. (3) In the WEPP, τ_c does not change with the variation of slope gradient (S) and hence is considered to be a constant [28]. Nevertheless, in developing a rational method for predicting τ_c, Lei et al. [29] suggested that τ_c increased when S changed from 0.087 to 0.423 and attributed this increase to the fact that the force along the slope enhanced when S was raised. Moreover, the critical shear stress of sediment particles in rivers mostly depended on bed S [30,31].

Due to the limitations of determining critical shear stress in rills by linear regression [32,33], some researchers have tried to determine critical shear stress by gradually increasing flow shear stress until an obvious detachment of soil particles is observed [34,35]. The critical shear stress of rill erosion determined by this method was called τ_o. Nouwakpo et al. [36] considered τ_c was not capable of detecting small variations in real critical shear stress because of its projected characteristic. Thus, they determined the τ_o of different hydraulic gradients and demonstrated a good linear relationship with the hydraulic gradient that was in line with the changing trend of K_r. Lei and Nearing [34] designed an apparatus to control flow discharge for well determining the τ_o of loose material. Although these studies presented satisfactory results, they only used the method of observing the initial detachment of soil particles to determine τ_o and did not compare these results with the widely used τ_c [17,21]. Thus, it is of paramount importance to investigate whether the method determining τ_o in rills is reliable.

Different from determining τ_o in rills, the method of determining critical shear stress in rivers by observing initial sediments has been extensively used [37–39], and a great deal of knowledge has been gained [40–42]. However, there are distinct discrepancies in hydraulic environments between rivers and rills [43]. Typical flow depths in rills are several centimeters or less, which is several orders of magnitudes lower than that of rivers [7]. The S of rivers was generally gentle (usually less than 0.01) [31], while it was steep for rills (up to 0.46) [44]. What is more, distinguishing differences exist between soils in rills and sediments in rivers [20,31]. Considering the great discrepancies between rivers and rills, the knowledge obtained from rivers may not be valid in rills [7,43]. Therefore, the reliability of the method determining τ_o in rills is in need of exploration.

For the purpose of exploring the reliability of the method determining τ_o in rills, undisturbed soils were preferable, considering the extrapolation of research results [24,45]. However, as mentioned above, K_r and τ_c of undisturbed soils were affected by numerous

soil properties and plant roots [17]. These influencing factors of K_r and τ_c were various, complicated, and, at times, greatly correlated [21]. Specifically designed experiments, which controlled influenced factors, were usually aimed at establishing an accurate relationship between K_r and τ_c and their influencing factors [21,27,46]. Clear relationships between τ_o and τ_c and their influencing factors were pivotal to estimating the reliability of the method determining τ_o. Disturbed soils, compared with undisturbed soils, could well control influencing factors, whereby the clear relationships between τ_o and τ_c and some fundamental factors (e.g., soil texture and SOM) could be more easily established with relatively lesser soil samples [24,47]. Therefore, disturbed soils, standing for the freshly tilled condition, were used in this study [21].

As mentioned earlier, a lot of disagreement exists regarding the usually used method (linear regression) to determine the critical shear stress of rills (τ_c), whereas the method measuring critical shear stress of rills by observing the start of soil particle detachment (τ_o) has shown promising results [36]. However, the reliability of the method determining τ_o was still unknown. Therefore, this study aimed to identify the reliability of the method determining τ_o in rills by comparing (1) the values of τ_o and τ_c, (2) the relationship between τ_o and τ_c, and K_r, and (3) the relationship between τ_o and τ_c and their influencing factors. This study's findings have important implications for recognizing rill erosion mechanisms and enhancing the prediction accuracy of erosion models.

2. Material and Methods

2.1. Soil Sampling

The Loess Plateau (total area of 6.2×10^5 km^2) is located in northwestern China. Irrational land use and low coverage of vegetation have made it the most severely eroded region in the world, and the soil erosion rate could be greater than 59,700 t km^{-2} yr^{-1} [48]. The Loess Plateau has a temperate and monsoon climate, with annual precipitation and mean temperature changes ranging from 800 mm to less than 200 mm and from 14.3 °C to 3.6 °C, respectively, from the south to the north. The vegetation zones change from forest to steppe desert from the south to the north [49]. Thick loess–paleosol deposits are distributed throughout the Loess Plateau. Clay loam is the most widespread soil, with soil texture becoming more sand and less clay from the south to the north [50]. Additionally, the SOM followed a decreasing trend from south to north [51]. From the south to the north, the decreasing clay content and SOM and the increasing sand content in this region would lead to an increase in K_r and possibly to the corresponding changes in τ_o and τ_c [21]. These influencing factors of K_r and τ_c also showed great variations from south to north [21], which was helpful for establishing accurate relationships between critical shear stresses and their influencing factors. Thus, a line transect with 330 km was laid out from the south to the north in this region (Figure 1). This transect has spread across three vegetation zones: forest, forest steppe, and steppe. Six sampling sites on this transect were chosen, and the interval of the two adjacent sampling sites was about 66 km (Figure 1 and Table 1). The southernmost sampling site was Yijun (a typical forest zone), and the northernmost sampling site was Yulin, the north part of which was the Mu Us desert.

Disturbed soils of cropland (20 cm) on the six sampling sites were selected from April to May 2019. On each sampling site, 100 kg of disturbed soils (top 20 cm of soil layer) were collected in 'S' shape (six soil samples). These soil samples were air-dried and sieved with a mesh aperture of 2 mm to simulate the freshly tilled condition [18,52]. A portion of these disturbed soils was used for the measurement of critical shear stress, and the other portion was used for the determination of soil properties.
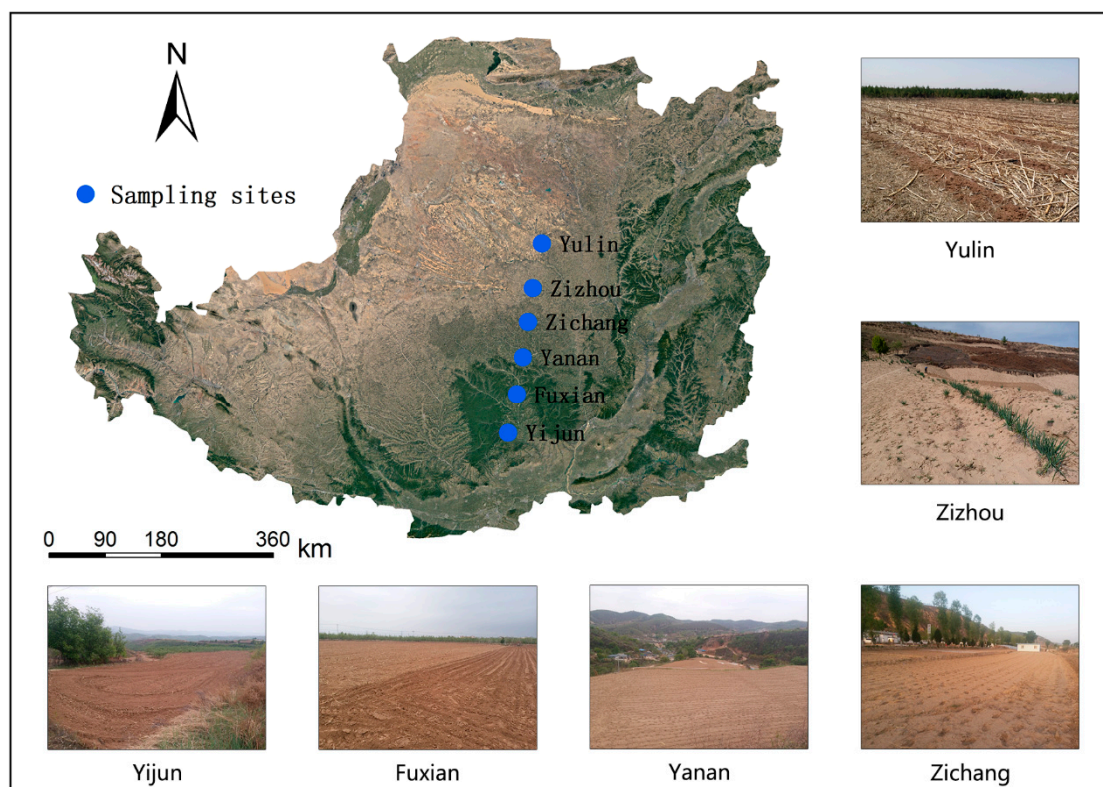
Figure 1. The six sampling sites.

Table 1. Description of six sampling sites.

Sampling Site	Longitude	Latitude	Elevation (m)	Temperature (°C)	Precipitation (mm)	Coverage (%)	Crop
Yijun	109°22′40″	35°23′22″	1002	10.3	591	1	Corn
Fuxian	109°27′19″	35°57′50″	1183	10.2	542	2	Corn
Yanan	109°34′34″	36°40′37″	980	9.9	514	5	Corn
Zichang	109°40′15″	37°10′31″	1058	9.6	437	3	Corn
Zizhou	109°44′19″	37°42′40″	1077	9.3	411	5	Corn
Yulin	109°48′10″	38°12′42″	1132	8.8	383	3	Corn

2.2. Determination of Critical Shear Stress

The water content (150 g kg^{-1}) of sieved soils was obtained by a sprinkling can, and the water was equilibrated for 24 h in a sealed plastic bucket. The same water content was used for the six sampling sites to reduce the effect of the water content and to fill the soil easily [21]. The wetted soils were put into a stainless-steel box (10 cm in diameter) in several steps. The bulk density of the samples from the six sampling sites was kept at 1.19 g kg^{-1} (i.e., the average bulk density of six sampling sites). For each sampling site, 60 soil samples were made, half of which was used for the determination of τ_c, and the other half was tested for τ_o. Altogether, 360 soil samples were collected for all six sampling sites. Before the measurement of critical shear stress, these soil samples were saturated for 12 h and then drained for 12 h.

τ_o was determined in a hydraulic flume (0.35 m in width, 5 m in length), which was described thoroughly in Su et al. [53]. To explore the effect of S on τ_o, six S (3.49%, 8.72%, 17.36%, 25.88%, 34.20%, and 42.26%) were set. On each S, τ_o was determined by gradually increasing the flow discharge until the continuous detachment of soil particles was observed [36,54]. A series of valves was employed to adjust the flow discharge (Q, m^3 s^{-1}). The increase of Q was stopped when the continuous detachment of soil particles occurred. The corresponding Q, flow velocity (V, m s^{-1}), and flow depth (H, m)

at this moment were termed as critical flow discharge (Q_o, m^3 s^{-1}), critical flow velocity (V_o, m s^{-1}), and critical flow depth (H_o, m). The measurements of Q_o, V_o, and H_o were the same as those obtained by Wang et al. [20] and Geng et al. [55], which have been thoroughly described. τ_o of each soil sample was calculated based on the following Equation (1):

$$\tau_o = \rho g H_o S \tag{1}$$

where ρ (kg m^{-3}) and g (m s^{-2}) are the water density and the gravity constant, respectively. The mean τ_o of five duplicates under the particular S was used. Table 2 lists the statistical characteristics of the noted hydraulic parameters.

Table 2. Critical hydraulic parameters for τ_o test of six sampling sites.

Items	Minimum	Maximum	Mean	Standard Deviation	CV
Q_o (m^3 s^{-1})	0.000040	0.000140	0.000065	0.000039	0.59
H_o (m)	0.00060	0.00133	0.00078	0.00028	0.35
V_o (m s^{-1})	0.18	0.25	0.21	0.03	0.13
τ_o (Pa)	1.08	1.78	1.34	0.24	0.18

Note: Q_o, critical flow discharge of τ_o test; H_o, critical flow depth of τ_o test; V_o, critical flow velocity of τ_o test; CV, coefficient of variance.

Similar to τ_o, τ_c was measured in the same hydraulic flume. The S was kept at a constant value (25.88%) to eliminate the influence of S. Six flow discharges ranging from 2.5×10^{-4} to 2.5×10^{-3} m^3 s^{-1} were applied to determine D_c. After the desired Q with an error of less than 2% was set, V and H were measured. The detailed measuring procedures of Q, V, and H were similar to Q_o, V_o, and H_o. τ of each flow discharge was calculated using Equation (1), but the difference was that τ_o and H_o were replaced by τ and H, respectively. The corresponding hydraulic parameters for each flow discharge are listed in Table 3. Then, the measurement of D_c was taken when the soil sample was put into the sample hole and was stopped when the scouring depth of 2 cm was exceeded. The scoured soil samples were oven-dried for 24 h (105 °C). D_c was calculated by the following equation:

$$D_c = \frac{M_i - M_f}{AT} \tag{2}$$

where M_i is initial dry soil mass; M_f is final dry soil mass; A is soil sample area; and T is scouring time. Five duplicates of each flow discharge were measured, and the mean values of five duplicates were used. K_r and τ_c were obtained by regressing six pairs of D_c and τ by Equation (3). The regressing slope and intercept on the *X*-axis were K_r and τ_c, respectively (Table 4).

$$D_c = K_r(\tau - \tau_c) \tag{3}$$

Table 3. Hydraulic parameters for τ_c test.

Q (m^3 s^{-1})	V (m s^{-1})	H (m)	τ (Pa)
0.00025	0.53	0.0014	3.45
0.0005	0.73	0.0020	5.00
0.001	1.01	0.0028	7.20
0.0015	1.26	0.0034	8.62
0.002	1.42	0.0040	10.22
0.0025	1.61	0.0044	11.26

Table 4. Calculated results of soil erosion resistance to overland flow of six sampling sites.

Sampling Sites	Regression Equations	R^2	NSE
Yijun	$D_c = 0.31 \, (\tau - 1.59)$	0.88	0.88
Fuxian	$D_c = 0.30 \, (\tau - 2.96)$	0.95	0.95
Yanan	$D_c = 0.33 \, (\tau - 2.44)$	0.98	0.98
Zichang	$D_c = 0.35 \, (\tau - 2.17)$	0.96	0.98
Zizhou	$D_c = 0.65 \, (\tau - 2.48)$	0.98	0.98
Yulin	$D_c = 1.97 \, (\tau - 3.65)$	0.98	0.97

So as to explore the influencing factors of τ_o and τ_c, some basic influencing factors (e.g., soil texture and SOM) were measured. The measurements of soil texture (e.g., clay content, silt content, and sand content) (two duplicates) and SOM (two duplicates) were taken by hydrometer and potassium dichromate colorimetric, respectively. The measured soil properties of six sampling sites are given in Table 5. As shown in Table 5, the clay content, silt content, and SOM generally followed decreasing trends from south to north, whereas sand content followed an increasing trend. Additionally, the soil properties of the six sampling sites presented great variations (Table 5).

Table 5. Soil properties of six sampling sites.

| Sampling Site	Clay Content (%)	Silt Content (%)	Sand Content (%)	SOM (g kg^{-1})
Yijun	10.11	77.36	12.53	12.37
Fuxian	9.47	76.66	13.87	12.69
Yanan	13.55	76.67	9.79	6.05
Zichang	11.56	62.33	26.11	6.37
Zizhou	5.43	39.97	54.60	1.19
Yulin	1.12	4.68	94.20	0.59

2.3. Data Analysis

All statistical analyses were conducted in SPSS 23.0. The difference between τ_o and τ_c was detected by the paired sample *t*-test. Pearson correlation analysis was applied to detect the relationship between measured soil properties and K_r, τ_o, and τ_c. Linear regression or nonlinear regression was applied to calculate K_r and τ_c and to analyze the relationships among S, soil properties, and τ_o. The coefficient of determination (R^2) and Nash–Sutcliffe efficiency (NSE) was employed to evaluate the fitness of the regressing results.

3. Results

### 3.1. Comparison of the Values of τ_o and τ_c

The minimum, mean, and maximum τ_c of the six sampling sites were 1.59 Pa, 2.55 Pa, and 3.65 Pa, respectively, while τ_o varied from 1.08 Pa to 1.78 Pa with a mean of 1.34 Pa. On average, the τ_c was 1.90 times greater than that of τ_o. τ_c and τ_o both showed moderate variability with a coefficient of variance (CV) of 0.25 and 0.16, respectively. As shown in Figure 2, the τ_c of all sampling sites was greater than τ_o, except for Yijun, where τ_o was only slightly greater than τ_c. The paired sample *t*-test also demonstrated a significant difference between τ_o and τ_c for six sampling sites ($p < 0.05$). Figure 2 shows that the changing trend of τ_c was chaotic from south to north. The two largest values appeared at Fuxian and Yulin, whereas the two lowest values appeared at Yijun and Zichang. From south to north, however, τ_o decreased gradually from Yijun (the maximum τ_o) to Zizhou (the minimum τ_o) and increased from Zizhou to Yulin.
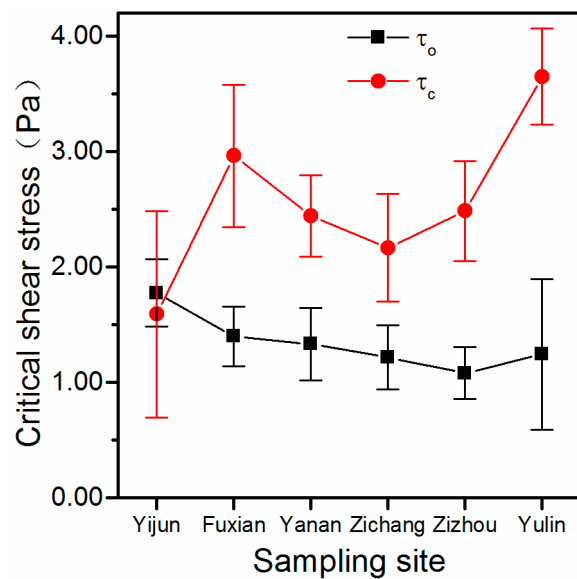
Figure 2. Comparison of critical shear stress determined by observed soil particles detachment (τ_o) and critical shear stress measured by linear regression (τ_c).

3.2. Comparison of the Relationship between τ_c and τ_o, and K_r

Table 4 lists the calculated results of K_r and τ_c, which showed satisfactory results with R^2 (0.88–0.98) and NSE (0.88–0.98). K_r generally followed an increasing trend from south to north (Figure 3). The increasing trend of K_r was associated with variations in soil texture (Table 6). K_r decreased with clay content and silt content, and it increased with sand content.
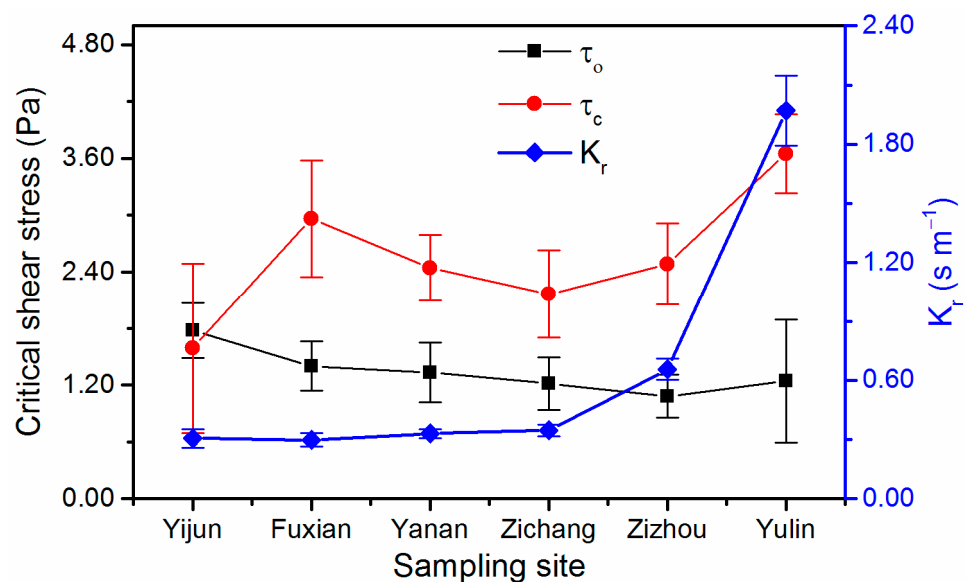
Figure 3. Comparison of the relationships between rill erodibility (K_r) and τ_o and τ_c.

Table 6. Relationship between Kr and soil properties by Pearson Correlation Coefficient.

Items	Clay Content (%)	Silt Content (%)	Sand Content (%)	SOM (g kg^{-1})
K_r	−0.884 *	−0.946 **	0.947 **	−0.687

Note: ** and * indicate significance at the 0.05 level and 0.01 level, respectively.

As shown in Figure 3, at the sampling site of Yulin, both K_r and τ_c had the maximum value. Yijun, however, had the lowest K_r and nearly the lowest τ_c. Fuxian had the lowest K_r and the second-largest τ_c. No significant relationship existed between K_r and τ_c since a very different changing trend was observed between τ_c and K_r (Figure 3). For the relationship between K_r and τ_o, from Yijun to Yulin, K_r and τ_o followed increasing and decreasing trends, respectively. From Zizhou to Yulin, however, both K_r and τ_o followed increasing trends.

3.3. Comparison of the Relationship between τ_c and τ_o, and Their Influencing Factors

The τ_c was independent of S in the WEPP model, and thus, only the influence of S on τ_o was evaluated. As shown in Figure 4, a significant positive relationship existed between τ_o and S, with R^2 ranging from 0.76 to 0.99 and NSE varying from 0.74 to 0.98. All sampling sites showed power functions between τ_o and S.
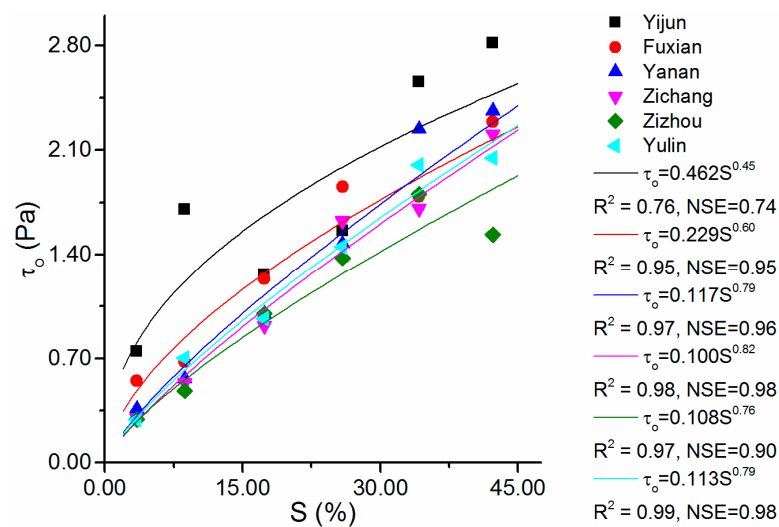

Figure 4. The relationship between τ_o and slope gradient (S).

Regarding the impact of soil properties on τ_o and τ_c, no significant relationship was found between τ_c and the measured soil properties. Similarly, no relationships existed among clay content, silt content, and sand content and τ_o. An exponential function of τ_o and SOM was expressed ($R^2 = 0.64$, NSE = 0.53; Figure 5).
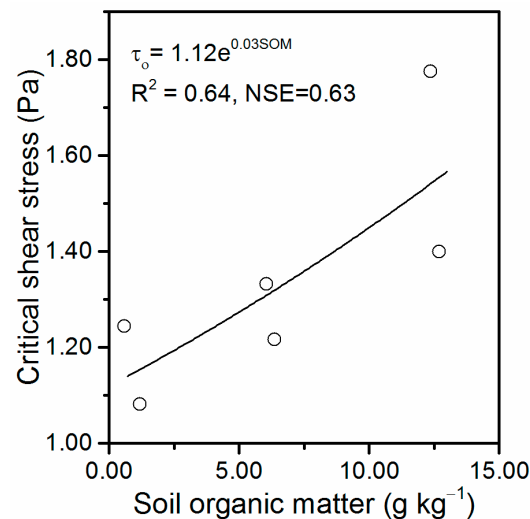

Figure 5. The relationship between τ_o and soil organic matter (SOM).

4. Discussion

Nearing et al. [12] defined τ_c as the threshold of rill detachment below in which soil detachment is zero. In this study, nearly all sampling sites had obviously greater τ_c than τ_o. Interestingly, an obvious soil detachment was apparent for sampling sites with higher τ_c, which might contradict the definition of τ_c [12]. This result meant that τ_c calculated by Equation (3) could not represent the critical condition of the start of soil detachment. The definition of τ_c has been contested [33,56]. For example, Knapen et al. [46] and Wang et al. [57] have stated that τ_c represented the appearance of significant detachment, which still did not explain why significant detachment was observed at the sampling sites with higher τ_c. Therefore, the reliability of τ_c determined by Equation (3) was probably controversial. Nearing et al. [32] also indicated τ_c had no actual meaning, as it was calculated by linear regression, and a large regression slope would lead to a large value (τ_c).

The gradually increasing trend of K_r could be well explained by the soil properties. Specifically, K_r was negatively correlated to clay content and silt content, and a positive relationship was observed between sand content and K_r (Table 6). This finding was consistent with the results of Geng et al. [21]. Some previous studies have shown K_r decreased with τ_c, implying that factors that influenced K_r also affected τ_c [58]. Although K_r showed an increasing trend from south to north and had a satisfactory relationship with soil properties, no significant relationship was observed between K_r and τ_c. Furthermore, Knapen et al. [59] indicated that the K_r of deep noninversion tillage was 10 times lower than that of conventional plowing, but the differences in τ_c between these two tillage practices were not significant. Additionally, Geng et al. [21] calculated K_r and τ_c of 36 soil types across eastern China and also found no significant relationship between K_r and τ_c. For the relationship between K_r and τ_o, K_r increased with an increase of τ_c from Yijun to Zizhou, which supported the perception that the higher τ_o corresponded to the lower K_r. The increasing trends of τ_o and K_r from Zizhou to Yunlin barely supported the inverse relationship between τ_o and K_r, which could be attributed to the low clay content and high sand content in Yulin (Table 5). Sand particles need higher flow shear stress to be detached because of their high ratio of mass to surface area [60]. Although Yulin has high τ_o, Yulin also showed high K_r. The low clay content of this sampling site may explain both the high K_r and τ_o of Yulin [21].

For τ_c, the widely applied WEPP model considered that τ_c did not change with the variation of S [14,25,34]. This study, however, found a significantly positive relationship between τ_o and S. This result was the opposite of the common-sense understanding that the gravitational force along a flume bed increases with S, which makes soil particles detach more easily [31]. Lei and Nearing [34] also found an increase of τ_o with S for loose material. In this study, the ratios of the H_o (S, 42.26%) to the H_o (S, 3.49%) for Yijun, Fuxian, Yanan, Zichang, Zizhou, and Yulin were 31.08%, 34.30%, 54.12%, 61.04%, 58.14%, and 58.37%, respectively. Nonetheless, the S (42.26%) was 12.11 times that of the S (3.49%). Thus, the influence of S on τ_o was much greater than H_o and explained why τ_o increased with S [34]. This statement was inconsistent with the findings of some researchers who found that the critical shear stress was related only to soil properties [25,28]. Nonetheless, hydraulic parameters and S also have been used to calculate the critical shear stress [24,61]. This discrepancy has probably reflected the lack of clarity regarding the significance of the critical shear stress [7].

Numerous disputes have existed with regard to the influence of soil properties on τ_c [21,24]. This study demonstrated a poor relationship between τ_c and measured soil properties. Our results, however, agreed with the findings of Geng et al. [21]. They explored the relationship between τ_c and 17 soil properties of 36 soil types and also did not find a significant relationship between τ_c and the 17 soil properties. For the relationship between τ_o and measured soil properties, τ_o increased exponentially and SOM (Figure 5), which agreed with the findings of Kimiaghalam et al. [62] and Grabowski et al. [63]. The poor relationship between τ_o and soil texture was probably caused by the fact that both the

cohesive effect of clay particles and the ratio of mass to surface area of sand particles determined τ_o, and their interaction was complicated [59].

Generally speaking, τ_o, compared with τ_c, did not present significantly better results with regard to the relationships with K_r, S, and soil properties. This finding could deepen the recognition of erosion processes and improve the precision of process-based soil erosion models. In this study, however, only the relationships between critical shear stress and some basic soil properties (soil texture and SOM) were established and compared, and the relationships with other key soil properties (such as soil cohesion, aggregate stability, plant root, etc.) were not investigated [64]. Therefore, further research should be conducted to compare the relationships between τ_o and τ_c and these influencing factors. Even though τ_o was more reliable compared to τ_c, observing the start of soil particle detachment was subjective [54]. Thus, it was meaningful to develop an objective method to ascertain the beginning of soil particle detachment [39,65]. Additionally, some researchers have argued that the critical shear stress had a relationship only with soil properties, which as well revealed the uncertainty of using a method to determine τ_o that was related to hydraulic parameters and S [28].

5. Conclusions

This study aimed to identify the reliability of critical shear stress in rills by observing the start of soil particle detachment. τ_c was determined by linear regression, and τ_o was measured by observing the soil particle detachment of six sampling sites along a transect of the Loess Plateau. The results showed that the mean τ_c (2.55 Pa) was 1.90 times that of τ_o (1.34 Pa). τ_c changed irregularly from south to north along the transect, and τ_o decreased from Yijun to Zizhou and then increased from Zizhou to Yulin. No significant relationship was observed between τ_c and rill erodibility (K_r). K_r increased with a decrease of τ_o from Yijun to Zizhou, whereas both K_r and τ_o followed increasing trends from Zizhou to Yulin. Although τ_c was deemed unchanged with S, τ_o followed an obviously increasing trend with the increase of S with great R^2 (0.76 to 0.99) and NSE (0.74 to 0.98). No significant relationship existed between τ_c and measured soil properties ($p > 0.05$); however, τ_o exhibited exponentially increasing functions with SOM ($R^2 = 0.64$; NSE = 0.63). Overall, τ_o displayed no significantly better results compared with τ_c, considering the relationships with K_r, S, and soil properties. Additionally, some uncertainties also remained regarding the method used to determine τ_o. The results of this study were helpful for the accurate measurement of critical shear stress in rills and for improving the prediction accuracy of the process-based soil erosion model.

Institutional Review Board Statement: Not applicable.

Informed Consent Statement: Not applicable.

Data Availability Statement: The data supporting the results of this study are available from the corresponding author on the condition of reasonable request.

Conflicts of Interest: The authors declare that they have no known competing financial interest or personal relationships that could have appeared to influence the work reported in this paper.

References

1. Stefanidis, S.; Alexandridis, V.; Ghosal, K. Assessment of Water-Induced Soil Erosion as a Threat to Natura 2000 Protected Areas in Crete Island, Greece. *Sustainability* **2022**, *14*, 2738. [CrossRef]
2. Orgiazzi, A.; Panagos, P. Soil biodiversity and soil erosion: It is time to get married: Adding an earthworm factor to soil erosion modelling. *Global Ecol. Biogeogr.* **2018**, *27*, 1155–1167. [CrossRef]
3. Li, Z.; Xu, X.; Zhu, J.; Xu, C.; Wang, K. Sediment yield is closely related to lithology and landscape properties in heterogeneous karst watersheds. *J. Hydrol.* **2019**, *568*, 437–446. [CrossRef]
4. Ma, Q.; Zhang, K.; Cao, Z.; Wei, M.; Yang, Z. Soil detachment by overland flow on steep cropland in the subtropical region of China. *Hydrol. Process.* **2020**, *34*, 1810–1820. [CrossRef]
5. Zhang, K.; Lian, L.; Zhang, Z. Reliability of soil erodibility estimation in areas outside the US: A comparison of erodibility for main agricultural soils in the US and China. *Environ. Earth Sci.* **2016**, *75*, 252. [CrossRef]
6. Trimble, S.W.; Crosson, P. US soil erosion rates—Myth and reality. *Science* **2000**, *289*, 248–250. [CrossRef]
7. Govers, G.; Giménez, R.; van Oost, K. Rill erosion: Exploring the relationship between experiments, modelling and field observations. *Earth Sci. Rev.* **2007**, *84*, 87–102. [CrossRef]
8. Lee, J.H.; Heo, J.H. Evaluation of estimation methods for rainfall erosivity based on annual precipitation in Korea. *J. Hydrol.* **2011**, *409*, 30–48. [CrossRef]
9. Li, P.; Mu, X.; Holden, J.; Wu, Y.; Irvine, B.; Wang, F.; Gao, P.; Zhao, G.; Sun, W. Comparison of soil erosion models used to study the Chinese Loess Plateau. *Earth Sci. Rev.* **2017**, *170*, 17–30. [CrossRef]
10. Chen, X.Y.; Huang, Y.H.; Zhao, Y.; Mo, B.; Mi, H.X.; Huang, C.H. Analytical method for determining rill detachment rate of purple soil as compared with that of loess soil. *J. Hydrol.* **2017**, *549*, 236–243. [CrossRef]
11. Nicosia, A.; Di Stefano, C.; Pampalone, V.; Palmeri, V.; Ferro, V.; Nearing, M.A. Testing a new rill flow resistance approach using the Water Erosion Prediction Project experimental database. *Hydrol. Process.* **2019**, *33*, 616–626. [CrossRef]
12. Nearing, M.A.; Foster, G.R.; Lane, L.J.; Finkner, S.C. A process-based soil erosion model for USDA-Water Erosion Prediction Project technology. *Trans. Am. Soc. Agric. Eng.* **1989**, *32*, 1587–1593. [CrossRef]
13. Al-Hamdan, O.Z.; Pierson, F.B.; Nearing, M.A.; Williams, C.J.; Stone, J.J.; Kormos, P.R.; Boll, J.; Weltz, M.A. Concentrated flow erodibility for physically based erosion models: Temporal variability in disturbed and undisturbed rangelands. *Water Resour. Res.* **2012**, *48*, W07504. [CrossRef]
14. Jiang, F.; He, K.; Huang, M.; Zhang, L.; Lin, G.; Zhan, Z.; Li, H.; Lin, J.; Ge, H.; Huang, Y. Impacts of near soil surface factors on reducing soil detachment process in benggang alluvial fans. *J. Hydrol.* **2020**, *590*, 25274. [CrossRef]
15. Ma, Q.; Zhang, K.; Jabro, J.D.; Ren, L.; Liu, H. Freeze–thaw cycles effects on soil physical properties under different de-graded conditions in Northeast China. Environ. *Earth Sci.* **2019**, *78*, 321. [CrossRef]
16. Sheridan, G.J.; So, H.B.; Loch, R.J.; Walker, C.M. Estimation of erosion model erodibility parameters from media properties. *Soil Res.* **2000**, *38*, 265–284. [CrossRef]
17. Knapen, A.; Poesen, J.; Govers, G.; Gyssels, G.; Nachtergaele, J. Resistance of soils to concentrated flow erosion: A review. *Earth Sci. Rev.* **2007**, *80*, 75–109. [CrossRef]
18. Geng, R.; Zhang, G.H.; Ma, Q.H.; Wang, H. Effects of landscape positions on soil resistance to rill erosion in a small catchment on the loess plateau. *Biosyst. Eng.* **2017**, *160*, 95–108. [CrossRef]
19. Fattet, M.; Fu, Y.; Ghestem, M.; Ma, W.; Foulonneau, M.; Nespoulous, J.; le Bissonnais, Y.; Stokes, A. Effects of vegetation type on soil resistance to erosion: Relationship between aggregate stability and shear strength. *Catena* **2011**, *87*, 60–69. [CrossRef]
20. Wang, B.; Zhang, G.H.; Shi, Y.Y.; Zhang, X.C. Soil detachment by overland flow under different vegetation restoration models in the Loess Plateau of China. *Catena* **2014**, *116*, 51–59. [CrossRef]
21. Geng, R.; Zhang, G.H.; Ma, Q.H.; Wang, L.J. Soil resistance to runoff on steep croplands in Eastern China. *Catena* **2017**, *152*, 18–28. [CrossRef]
22. De Baets, S.; Poesen, J.; Knapen, A.; Galindo, P. Impact of root architecture on the erosion-reducing potential of roots during concentrated flow. *Earth Surf. Process. Landf.* **2007**, *32*, 1323–1345. [CrossRef]
23. Nearing, M.A.; Bradford, J.M.; Parker, S.C. Soil detachment by shallow flow at low slopes. *Soil Sci. Soc. Am. J.* **1991**, *55*, 339–344. [CrossRef]
24. Wirtz, S.; Seeger, M.; Remke, A.; Wengel, R.; Wagner, J.F.; Ries, J.B. Do deterministic sediment detachment and transport equations adequately represent the process-interactions in eroding rills? An experimental field study. *Catena* **2013**, *101*, 61–78. [CrossRef]
25. Gilley, J.E.; Elliot, W.J.; Laflen, J.M.; Simanton, J.R. Critical shear stress and critical flow rates for initiation of rilling. *J. Hydrol.* **1993**, *142*, 251–271. [CrossRef]
26. Foster, G.R. Modeling the erosion process. In *Hydrologic Modeling of Small Watersheds*; ASAE Monograph No. 5.; Haan, C.T., Ed.; American Society of Agricultural Engineers: St. Joseph, MI, USA, 1982; pp. 296–380.
27. Mamo, M.; Bubenzer, G.D. Detachment rate, soil erodibility, and soil strength as influenced by living plant roots part I: Laboratory study. *Trans. Am. Soc. Agric. Eng.* **2001**, *44*, 1167. [CrossRef]
28. Flanagan, D.C.; Nearing, M.A. *USDA-Water Erosion Prediction Project: Hillslope Profile and Watershed Model Documentation*; Nserl Rep, 10; USDA-ARS National Soil Erosion Research Laboratory: West Lafayette, IN, USA, 1995; pp. 1–123.
29. Lei, T.W.; Zhang, Q.W.; Yan, L.J.; Zhao, J.; Pan, Y.H. A rational method for estimating erodibility and critical shear stress of an eroding rill. *Geoderma* **2008**, *144*, 628–633. [CrossRef]

30. Dey, S.; Debnath, K. Influence of streamwise bed slope on sediment threshold under stream flow. *J. Irrig. Drain Eng.* **2000**, *126*, 255–263. [CrossRef]
31. Lamb, M.P.; Dietrich, W.E.; Venditti, J.G. Is the critical Shields stress for incipient sediment motion dependent on chan-nel-bed slope? *J. Geophys. Res.* **2008**, *113*, F2. [CrossRef]
32. Nearing, M.A.; Lane, L.J.; Lopes, V.L. Modeling soil erosion. In *Soil Erosion Research Methods*, 2nd ed.; Lal, R., Ed.; Soil and Water Conservation Society and St. Lucie Press: Delray Beach, FL, USA, 1994; pp. 127–156.
33. Zhu, J.C.; Gantzer, C.J.; Anderson, S.H.; Peyton, R.L.; Alberts, E.E. Comparison of concentrated-flow detachment equations for low shear stress. *Soil Tillage Res.* **2001**, *61*, 203–212. [CrossRef]
34. Lei, T.W.; Nearing, M.K. Laboratory experiments of rill initiation and critical shear stress in loose soil material. *Trans. Chin. Soc. Agric. Eng.* **2000**, *16*, 26–30, (In Chinese with English Abstract).
35. Wang, C.; Wang, B.; Wang, Y.; Wang, Y.; Zhang, W.; Yan, Y. Impact of near-surface hydraulic gradient on the interrill erosion process. *Eur. J. Soil Sci.* **2020**, *71*, 598–614. [CrossRef]
36. Nouwakpo, S.K.; Huang, C.H.; Bowling, L.; Owens, P. Impact of vertical hydraulic gradient on rill erodibility and critical shear stress. *Soil Sci Soc. Am. J.* **2010**, *74*, 1914–1921. [CrossRef]
37. Lavelle, J.W.; Mofjeld, H.O. Do critical stresses for incipient motion and erosion really exist? *J. Hydraul. Eng.* **1987**, *113*, 70–385. [CrossRef]
38. Buffington, J.M.; Dietrich, W.E.; Kirchner, J.W. Friction angle measurements on a naturally formed gravel streambed: Implications for critical boundary shear stress. *Water Resour. Res.* **1992**, *28*, 411–425. [CrossRef]
39. Righetti, M.; Lucarelli, C. May the Shields theory be extended to cohesive and adhesive benthic sediments? *J. Geophys. Res.* **2007**, *112*, C5. [CrossRef]
40. Buffington, J.M. The legend of AF Shields. *J. Hydraul. Eng.* **1999**, *125*, 376–387. [CrossRef]
41. García, M.H. Discussion of The Legend of AF Shields. *J. Hydraul. Eng.* **2000**, *126*, 718–720. [CrossRef]
42. Zhang, M.; Yu, G. Critical conditions of incipient motion of cohesive sediments. *Water Resour. Res.* **2017**, *53*, 7798–7815. [CrossRef]
43. Nearing, M.A.; Norton, L.D.; Bulgakov, D.A.; Larionov, G.A.; West, L.T.; Dontsova, K.M. Hydraulics and erosion in eroding rills. *Water Resour. Res.* **1997**, *33*, 865–876. [CrossRef]
44. Shi, Z.H.; Fang, N.F.; Wu, F.Z.; Wang, L.; Yue, B.J.; Wu, G.L. Soil erosion processes and sediment sorting associated with transport mechanisms on steep slopes. *J. Hydrol.* **2012**, *454*, 123–130. [CrossRef]
45. Giménez, R.; Govers, G. Flow detachment by concentrated flow on smooth and irregular beds. *Soil Sci. Soc. Am. J.* **2002**, *66*, 1475–1483. [CrossRef]
46. Knapen, A.; Poesen, J.; Govers, G.; de Baets, S. The effect of conservation tillage on runoff erosivity and soil erodibility during concentrated flow. *Hydrol. Process.* **2008**, *22*, 1497–1508. [CrossRef]
47. Stroosnijder, L. Measurement of erosion: Is it possible? *Catena* **2005**, *64*, 162–173. [CrossRef]
48. Geng, R.; Zhang, G.H.; Hong, D.L.; Ma, Q.H.; Jin, Q.; Shi, Y.Z. Response of soil detachment capacity to landscape positions in hilly and gully regions of the Loess Plateau. *Catena* **2021**, *196*, 104852. [CrossRef]
49. Liu, Z.P.; Shao, M.A.; Wang, Y.Q. Spatial patterns of soil total nitrogen and soil total phosphorus across the entire Loess Plateau region of China. *Geoderma* **2013**, *197*, 67–78. [CrossRef]
50. Yang, Y.; Jia, X.; Wendroth, O.; Liu, B.; Shi, Y.; Huang, T.; Bai, X. Noise-assisted multivariate empirical mode decomposition of saturated hydraulic conductivity along a south-north transect across the Loess Plateau of China. *Soil Sci. Soc. Am. J.* **2019**, *83*, 311–323. [CrossRef]
51. Liu, Z.P.; Shao, M.A.; Wang, Y.Q. Large-scale spatial variability and distribution of soil organic carbon across the entire Loess Plateau, China. *Soil Res.* **2012**, *50*, 114–124. [CrossRef]
52. Liu, H.; Wang, J.; Zhang, K.; Kong, Y. Effectiveness of geotextiles for road slope protection under simulated rainfall. *Environ. Earth Sci.* **2016**, *75*, 1–11. [CrossRef]
53. Su, Z.-L.; Zhang, G.-H.; Yi, T.; Liu, F. Soil Detachment Capacity by Overland Flow for Soils of the Beijing Region. *Soil Sci.* **2014**, *179*, 446–453. [CrossRef]
54. Salem, H.; Rennie, C.D. Practical determination of critical shear stress in cohesive soils. *J. Hydraul. Eng.* **2017**, *143*, 04017045. [CrossRef]
55. Geng, R.; Zhang, G.H.; Li, Z.W.; Wang, H. Spatial variation in soil resistance to flowing water erosion along a regional transect in the Loess Plateau. *Earth Surf. Process. Landf.* **2015**, *40*, 2049–2058. [CrossRef]
56. Khanal, A.; Klavon, K.R.; Fox, G.A.; Daly, E.R. Comparison of linear and nonlinear models for cohesive sediment detachment: Rill erosion, hole erosion test, and streambank erosion studies. *J. Hydraul. Eng.* **2016**, *142*, 04016026. [CrossRef]
57. Wang, J.G.; Li, Z.X.; Cai, C.F.; Yang, W.; Ma, R.M.; Zhang, G.B. Predicting physical equations of soil detachment by simulated concentrated flow in Ultisols (subtropical China). *Earth Surf. Process. Landf.* **2012**, *37*, 633–641. [CrossRef]
58. Nearing, M.A.; West, L.T.; Brown, L.C. A consolidation model for estimating changes in rill erodibility. *Trans. Am. Soc. Agric. Eng.* **1988**, *31*, 696–700.
59. Knapen, A.; Poesen, J.; de Baets, S. Seasonal variations in soil erosion resistance during concentrated flow for a lo-ess-derived soil under two contrasting tillage practices. *Soil Tillage Res.* **2007**, *94*, 425–440. [CrossRef]
60. Poesen, J.; de Luna, E.; Franca, A.; Nachtergaele, J.; Govers, G. Concentrated flow erosion rates as affected by rock fragment cover and initial soil moisture content. *Catena* **1999**, *36*, 315–329. [CrossRef]

61. De Ploey, J. Threshold conditions for thalweg gullying with special reference to loess areas. *Catena* **1990**, *17*, 147–151.
62. Kimiaghalam, N.; Clark, S.P.; Ahmari, H. An experimental study on the effects of physical, mechanical, and electro-chemical properties of natural cohesive soils on critical shear stress and erosion rate. *Int. J. Sediment. Res.* **2016**, *31*, 1–15. [CrossRef]
63. Grabowski, R.C.; Droppo, I.G.; Wharton, G. Erodibility of cohesive sediment: The importance of sediment properties. *Earth Sci. Rev.* **2011**, *105*, 101–120. [CrossRef]
64. Vannoppen, W.; Vanmaercke, M.; de Baets, S.; Poesen, J. A review of the mechanical effects of plant roots on concentrated flow erosion rates. *Earth Sci. Rev.* **2015**, *150*, 666–678. [CrossRef]
65. Ternat, F.; Boyer, P.; Anselmet, F.; Amielh, M. Erosion threshold of saturated natural cohesive sediments: Modeling and experiments. *Water Resour. Res.* **2008**, *44*, W11434. [CrossRef]